Journal of Structural Geology 26 (2004) 1647–1657

JOURNAL OF STRUCTURAL GEOLOGY

www.elsevier.com/locate/jsg

Emplacement and fabric-forming conditions of the Alous-En-Tides granite, eastern border of the Tin Seririne/Tin Mersoï basin (Algeria): magnetic and visible fabrics analysis

Bernard Henry[a,*], Hamou Djellit[b], Boualem Bayou[b], Mohamed E.M. Derder[b], Aziouz Ouabadi[c], Mounir K. Merahi[b], Kamal Baziz[d], Allaoua Khaldi[e], Abderahmane Hemmi[b]

[a]*Géomagnétisme et Paléomagnétisme, IPGP and CNRS, 4 avenue de Neptune, 94107 Saint-Maur cedex, France*
[b]*CRAAG, BP 63, 16340 Bouzaréah, Alger, Algeria*
[c]*FSTGAT/USTHB, BP 32, El-Alia Bab Ezzouar, 16111 Alger, Algeria*
[d]*ENOR, BP 44, Tamanrasset, Algeria*
[e]*CRND, BP 43, Sebala, Draria, Algeria*

Received 24 March 2003; received in revised form 2 February 2004; accepted 4 February 2004

Available online 11 March 2004

Abstract

The Alous-En-Tides pluton intruded within one of the most important Late Panafrican N–S shear zones, the 7°30 shear zone in the southern Hoggar shield. A magnetic fabric study points out strong preferred orientations of the magnetite grains. The orientation is coherent in the whole massif. However it cannot be correlated with any of the visible structures in the field or in thin section. Strongly oriented magnetites are thus disseminated within all the rock. The main rock-forming minerals in this pluton were not preferably oriented during their crystallization, showing that magma was emplaced without strongly oriented stresses. Magnetite orientations on the contrary reflect a strong stress field. Strike-slip movements along the 7°30 shear zone probably generated local relative distension, allowing pluton emplacement. During the last magmatic phase, they put the intrusion under the regional compressional stress field, causing orientation of the magnetite. The magnetic fabric then reveals the regional ENE–WSW stress field during Late Panafrican times. In part of the pluton, which was later affected by very intense solid-state deformation during dextral movement, the magnetic fabric remains mainly in connection with this initial magnetite fabric.

Keywords: Magnetic fabric; Granite; Shear zone; Late Panafrican; Hoggar shield

1. Introduction

In the southern part of the Hoggar shield, the limit between Sérouénout and Assodé–Issalane terranes (Black et al., 1994) corresponds to one of the main N–S Panafrican structures: the 7°30 shear zone (Bertrand et al., 1978; Caby et al., 1981; Caby, 1987). This shear zone appears in the field as a very large faulted zone, with extremely intense mylonitization. Close to the eastern limit of the Tin Seririne/Tin Mersoï Paleozoic basin, a late Panafrican granitic pluton (Baziz, pers. comm.) emplaced in the basement is located at Alous-En-Tides within this 7°30 zone and its western border (Fig. 1). It is totally mylonitized within the faulted zone, has visible strong N–S vertical foliation and horizontal lineation very close to this zone, but seems massive farther from it. The aim of this study is to point out the structural relations between this pluton and the 7°30 shear zone, during and after granite emplacement.

2. Geological setting and sampling

The Hoggar, also called the 'Touareg' or 'Targui' shield, consists of meso-catazonal series of Archean, Eburnean and Neoproterozoic material, cut by granites. The Neoproterozoic Pan-African belts results from its collision with the West African craton, which borders it to the West.

The Hoggar is subdivided into three main domains

* Corresponding author. Tel.: +33-1-4511-4180; fax: +33-1-4511-4190. *E-mail address:* henry@ipgp.jussieu.fr (B. Henry).

0191-8141/$ - see front matter © 2004 Elsevier Ltd. All rights reserved.
doi:10.1016/j.jsg.2004.02.003

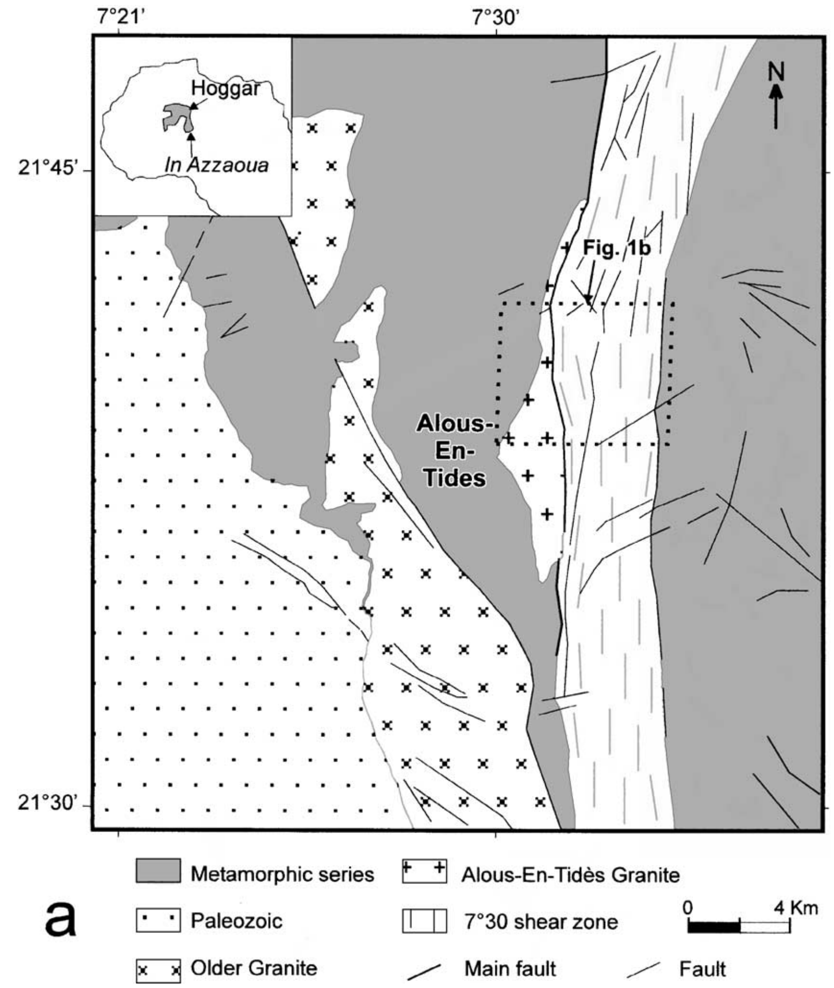

Fig. 1. (a) The 7°30 faulted zone and the Alous-En-Tides pluton in the Hoggar area. (b) Sampling sites of granite (sites G).

(Lelubre, 1952) separated by the mylonitic sub meridian mega-shear zones of the '4°50' and the '8°30'. The *central Hoggar*, within which is located the studied pluton, is mainly constituted of Eburnean gneiss, 'tectonized' during the Pan-African times and cut by several granites.

In more detail, the Hoggar is subdivided by several N–S shear zones into 23 terranes (Black et al., 1994), each of them with their own lithologies, tectonics and magmatism. These terranes were assembled during the Pan-African orogeny (between 750 and 550 Ma). The period between 650 and 550 Ma is mainly characterized by horizontal movements along mega-shear zones, and by emplacement of high-K calc–alkaline granitoids, locally followed by an alkaline–peralkaline magmatism.

The present study area is located around the '7°30' shear zone, which is the limit between the 'Assodé–Issalane' and the 'Sérouénout' terranes. The 'Assodé–Issalane' terrane is constituted of gneiss, from widespread anatexy and with upper amphibolite facies. It includes old basement, several supra-crustal sequences, alkalic gneiss, anatectic potassic granite (670 Ma) and high-K calc–alkalic granitoids (645–580 Ma). The 'Sérouénout' terrane is constituted of gneiss retro-morphosed into upper amphibolite facies, graphitic aluminous micaschist, foliated granodiorite, and high-K calc–alkalic granitoids (580 Ma).

Overlying uncomformably the meso-catazonal series in the terranes are Cambrian molasses ('séries pourprées' type; Caby, 1967; Caby and Moussu, 1967; Djellit et al., 2002) and/or Ordovician to Permian , which have been deposited, mainly with clays and sandstones and reaching locally 10 km thickness.

In the Tin Sirririne region, this series forms a synclinal structure extending northwards (on the Algerian territory), the Tin Mersoï basin, which has a broad extent around the Niger, South East of Hoggar.

This structure is a large depression having an almost flat bottom except close to its western border, which dips steeply (dip reaching 60°) close to a fault network of nearly N–S strike (faults of In Guezzam promontory).

The polyphased evolution of the 7°30 shear zone, mainly characterized by dextral strike-slip movements, began before and continued after intrusion of the Alous-En-Tides granite. The subject of this paper corresponds to only a part of this evolution.

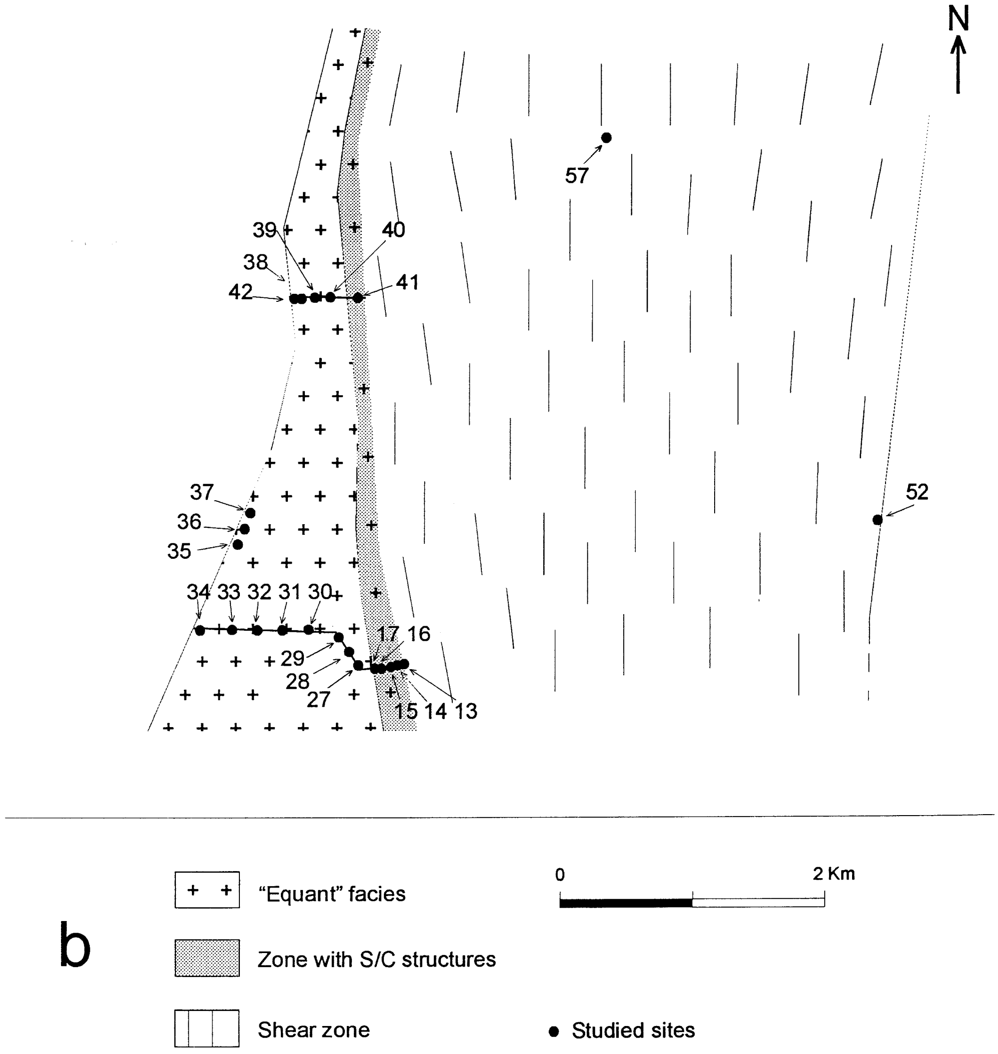

Fig. 1 (*continued*)

The host rocks of the studied pluton are mainly other granites or metamorphic rocks of Panafrican age or older. Because of outcrop conditions, the contact between the studied pluton and these host rocks cannot be directly observed. The older granites and metamorphic rocks are often cut by undeformed (except close to the 7°30 structure) doleritic dykes, which formed after the main Panafrican orogeny. The dykes were never observed within the studied pluton, though several of them have been found very close to this pluton and should have cut it with respect to their orientation. In addition, enclaves observed within the pluton correspond sometimes to dolerites. The pluton is therefore more recent than these dykes.

The Paleozoic series of the Tin Seririne/Tin Mersoï basin (Joulia, 1959), dated at their bottom of lower Ordovician age, crops out a few kilometers to the west of the pluton, with a very gentle dip of the sedimentary layering. According to this dip and the altitude of the top of the pluton, it was directly overlying the studied granite before it was eroded. In addition, within the basement outcrops, at about 5 km from the Tin Seririne basin border, an isolated but relatively large outcrop of the Ordovician formation has been observed within the 7°30 zone, which therefore corresponded to a graben during part of its evolution after the deposition of the Ordovician formation. It overlies locally the Alous-En-Tides granite, being separated from it by red granite wash and sand.

A long period of erosion of several kilometers of rock therefore occurred between pluton emplacement and deposition of the Paleozoic series. Cambrian 'Intermediate series' (Caby, 1967), observed west of the Tin Seririne basin (Djellit et al., 2002), seems not to presently exist in the studied area or they can be represented only by the red granite wash and sand. All these indications point out a Late Panafrican age for the pluton. This granite should be therefore the equivalent of some plutons of the Aïr (Liégeois et al., 1994) and of some Taourirt and other Late Panafrican granites (Lelubre, 1952; Boissonnas, 1973) in the northern and central part of the Hoggar, which are dated around 590–525 Ma (Boissonnas et al., 1964; Cahen et al., 1984;

Cheilletz et al., 1992; Paquette et al., 1998). An age of 570 ± 20 Ma (Liégeois and Baziz, pers. comm.) has been determined in a circular pluton, very similar to the Alous-En-Tides pluton and located 60 km southeast (at 7°50′ E, 21°15′ N) from the latter.

The late Panafrican Alous-En-Tides granites consist of perthitic K-feldspath transformed into microcline in the most deformed area, quartz, plagioclase (An_{8-13}), rare Fe rich biotite ($X_{fe} = 0.78$) partially pseudomorphosed to chlorite with accessory magnetite and allanite. The rocks are slightly peraluminous high-K calc–alkaline syenogranite ($SiO_2 = 74$–76%, molar ratio A/CNK > 1). The granites are all ($K_2O + Na_2O$) rich (>8%) and depleted in MgO (<0.23%). Major elements are in agreement with those of highly fractionated calc–alkaline rock types. These granites have a similar chemical composition both in the faulted area (near the 7°30 shear zone) and in the apparently undeformed western areas.

From the structural point of view, the granites are strongly deformed and present a strong fabric near the shear zone. The deformation decreases as one moves away from the shear zone and the granite appears in the field without the preferred orientation of its main minerals in most of the outcrops.

In thin sections, the granite is, however, deformed everywhere in the studied area:

(i) Far from the shear zone, its deformation is expressed by a strong cataclasis of the minerals such as fractured feldspar and micas (kink bands, mechanical twins), stretched with mylonitic spaced foliation planes. Few opaque minerals are visible within the S foliation. Rare C planes are only hinted at by a weak curvature of quartz ribbons.

(ii) Near the shear zone, in the deformed facies (Fig. 1b), the granite shows clear tectonic structures (S/C type composite foliation and horizontal extension lineation), lepidoblastic textures strongly oriented (quartz in tablet with strongly shape preferential orientation typical of ductile mylonite). The reduction of the grain size of the main minerals, comparative with those of the cataclasized granite, is in agreement with an important dynamic recrystallization and strain increase. The S foliation is vertical and trends N–S, and the vertical C planes trends NNE–SSW. The visible extension lineation is mostly horizontal and N–S-trending. This geometric relation between S and C planes is in agreement with dextral movements. Opaque minerals, though in relatively small amounts, underline the S planes, and to a lesser extent the C planes. The opaque minerals associated with the latter are sometimes distorted by shearing along the C planes.

Within the mylonitized zone, the S foliation and the lineation are locally folded about a steeply plunging fold axis. Bad outcrop conditions do not allow the precise determination of the orientation of the fold axis or specification of whether the strike-slip displacements were dextral or sinistral. Moreover, everywhere in the pluton, a more recent brittle deformation is characterized by sinistral NNW–SSE and dextral NE–SW fractures related to an E–W compressional stress field.

For simplification, granite without clear preferred orientation will be referred to here as undeformed, through the cataclasis of its main minerals.

The sampling sites (Fig. 1b) were mostly concentrated along two E–W cross-sections, perpendicular to the 7°30 shear zone. The aim of this work is not to map the magnetic fabric in the whole massif, but to study the variations of this fabric from the shear zone to the apparently undeformed western areas. One of the cross-sections is close to the widest part of the massif and the other, in contrast, is in an area where the granite at the west of the shear zone is reduced to a few hundreds of meters. Because of extreme mylonitization, only one site (57G), corresponding to a very small outcrop—about 2 m^2—partly mylonitized, has been found within the faulted zone and another on the eastern border of this zone. Finally, to have more data about the fabrics near the contact with host rocks, three additional sites were chosen, between the two cross-sections, as close as possible to the western border of the massif, two of these sites being separated by a few meters but corresponding to different intrusive facies (granite and granodiorite).

3. Rock magnetic data

Thermomagnetic analyses of low field magnetic susceptibility (K) were done on an Agico KLY3 susceptibility bridge with high and low temperatures attachments. Curves for high temperatures (Fig. 2a) point out moderate mineralogical alteration during heating. They show mainly a sharp decrease of susceptibility at 580 °C, which is the Curie temperature of pure magnetite. Verwey transition is a change of mineralogical phase, characterizing Ti-poor titanomagnetite, occurring at −180 °C and corresponds to a variation of magnetic susceptibility. It clearly appears on susceptibility curves for low temperature of Alous-En-Tides samples (Fig. 2b). The magnetic carrier is therefore pure magnetite. The characteristic rectangular shape of the high temperature thermomagnetic curve and the absence of well expressed Hopkinson peaks (on the thermomagnetic curve for temperature immediately below the Curie temperature, increase the magnetic susceptibility occurring for particular grain sizes of ferromagnetic minerals) suggest that the magnetite is of large multi-domain (MD) size in the Alous-En-Tides samples. Hysteresis loops were generated using a translation inductometer within an electromagnet capable of reaching 1.6 T. The analysis of the corresponding hysteresis parameters (Day et al., 1977) allows the determination of the

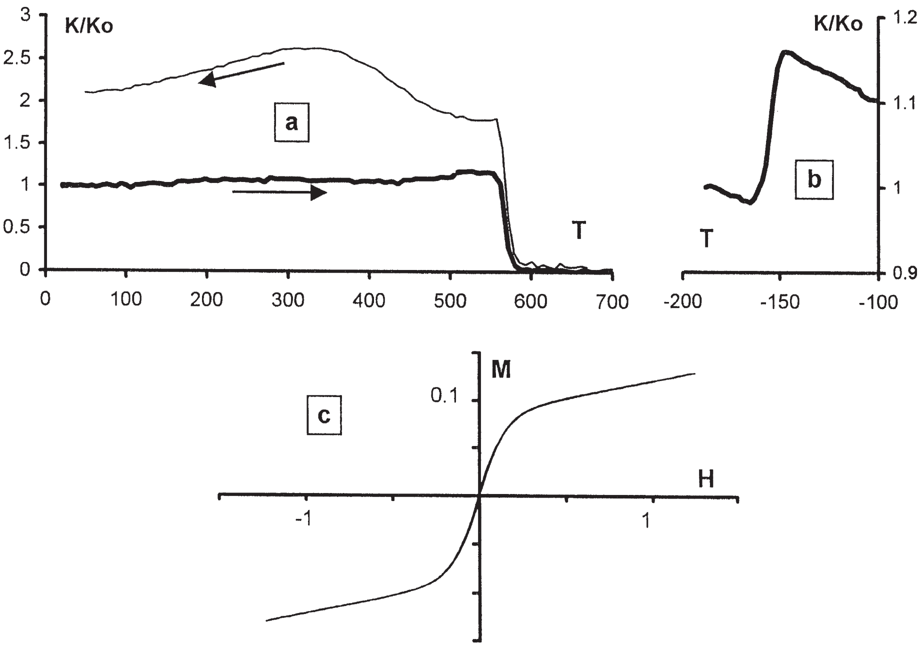

Fig. 2. Thermomagnetic curve (normalized susceptibility K/K_o as a function of temperature T in °C) for high (a) and low (b) temperatures. (c) Hysteresis loop (M in A m^2/kg, H in Tesla): $J_{rs}/J_s = 0.035$, $H_{cr}/H_c = 5.82$.

mean size of ferromagnetic grains. Obtained curves (Fig. 2c) point out only low coercive forces magnetic minerals. It confirms that the magnetite grains of the Alous-En-Tides granite have here large MD size. We can thus expect fabric directly related to shape anisotropy of the magnetite grains.

4. Magnetic fabric data

Anisotropy of magnetic susceptibility in a low field was measured using the KLY3 susceptibility bridge. The Jelinek (1981) parameters P' and T were used to describe the scalar magnetic fabric data. Data for a group of samples were analyzed using classical tensor variability statistics (Hext, 1963; Jelinek, 1978). The magnetic zone axis (Henry, 1997), corresponding to the mean axis of variation of the magnetic foliation plane in a group of samples, was determined. Orientation comparison between the magnetic zone axis and the magnetic lineation yields information about the structural significance of the magnetic lineation.

K values are mostly relatively high, on the order of some 10^{-3} SI (Fig. 3), indicating magnetic fabric mainly carried by magnetite. The highest K values were obtained on the western border of the pluton. Sites within or close to the

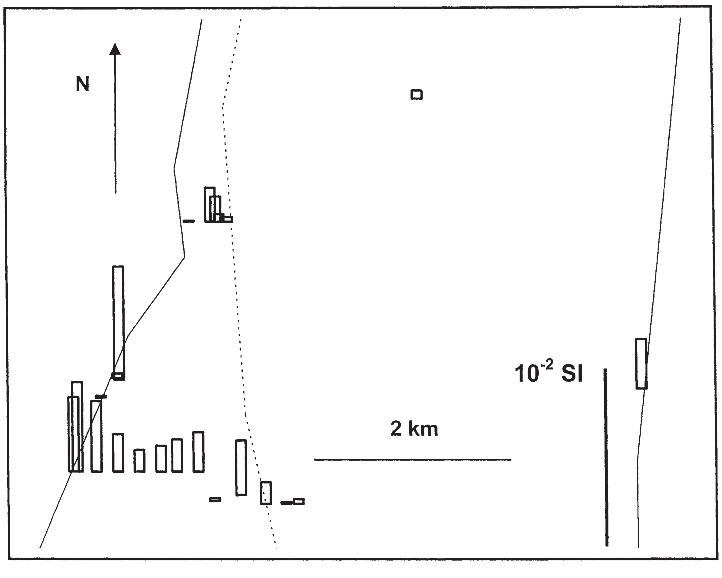

Fig. 3. Susceptibility (K) values.

shear zone have relatively low susceptibility values. This suggests, for this zone, either that part of the magnetite was destroyed or that initial rock composition was different for the opaque minerals. For the two neighboring sites with different magmatic rock types, susceptibility is much lower in the granodiorite facies than in the granite one. The magnetic fabric (Table 1) appears to be coherent in the whole massif, except for the site within the faulted zone (site 57G), which will be considered independently.

4.1. All sites except site 57G

Minimum axes are well clustered around a WSW-trending gently plunging orientation (Fig. 4b and c). Maximum axes are mainly well grouped, with an average NNW trend and a shallow plunge (Fig. 4a). Few maximum axes correspond to a girdle perpendicular to the minimum axes. The mean orientation of maximum axes (Fig. 4a and c) is very well defined, with a very small confidence zone. It coincides with the magnetic zone axis (Fig. 4d), and could be therefore an intersection lineation as well as an extension lineation. On a map, the orientations of the mean magnetic foliation and lineation per site appear to be independent of the site location, except for a weak deviation towards a N–S trend in the deformed granite (Fig. 5). On the western border of the pluton, the orientation of the magnetic foliation is different from that of the contact with host rocks. It is the same in granitic and granodioritic facies.

P' values for most of the samples are between 1.03 and 1.20 and the fabric is mostly oblate (Fig. 6a). All samples displaying P' values higher than 1.20 have an oblate fabric. Low P' values often correspond to low susceptibility values, and are not therefore indicating fabric with a significantly lower degree of preferred orientation of the minerals (Henry, 1980). On a map (Fig. 7), P' values are relatively coherent in the whole massif. T parameter values mostly indicate the strongest flattening in the borders of the shear zone. On the other hand, sites with a slightly prolate fabric correspond mainly to the same area, close to the western border of the pluton, but for most of the other sites within the pluton, the fabric is only slightly oblate and in general the shape of the fabric appears as almost homogeneous in areas not close to the faulted zone.

4.2. Site 57G

The visible structures in site 57G are similar to that observed on the border of the shear zone (clear visible foliation and lineation), but they were in addition relatively intensively deformed by local folding related to late strike-slip displacements of the shear zone.

P' and T values in site 57G within the shear zone have some similar characteristics (Figs. 6b and 8) as in sites on the borders of this zone: oblate fabric and similar P' values as in the other sites. The minimum axes (Fig. 8a) are a little more scattered than in the other sites, and the associated

Table 1
For the different sites, number of samples (*N*), mean susceptibility *K* (10^{-6} SI), Declination *D* and inclination *I* (in degrees) for mean maximum susceptibility axis (Max), mean visible lineation (*L*), mean minimum susceptibility axis (Min), pole of the mean visible foliation (*F*), P' and *T* parameters. Values in brackets correspond to badly defined orientations

Site	*N*	*K*	Max		*L*		Min		*F*		P'	*T*
			D	*I*	*D*	*I*	*D*	*I*	*D*	*I*		
13G	9	268	345	53			81	5	84	0	1.08	0.65
14G	6	105	352	35			259	5	88	0	1.07	0.65
15G	6	1227	336	8			67	13	(82)	(15)	1.12	0.72
16G	6	3077	162	3			72	8			1.18	0.23
17G	6	160	344	34			251	5			1.06	0.36
27G	7	2195	348	15			256	5			1.14	0.35
28G	6	1797	334	16			240	15			1.10	0.30
29G	6	1452	347	22			252	11			1.11	0.17
30G	11	1216	152	26			249	13			1.07	0.81
31G	7	2077	340	44			236	13			1.14	0.36
32G	6	3965	339	15			240	28			1.16	−0.12
33G	8	5024	356	38			249	21			1.12	−0.32
34G	8	4193	352	29			256	10			1.14	−0.01
35G	8	103	337	21			242	13			1.04	0.23
36G	6	252	357	14			264	13			1.04	0.09
37G	7	6449	1	11			267	22			1.26	0.57
38G	6	1922	325	4			54	10			1.13	−0.04
39G	5	1430	328	7			59	10	(270)	(15)	1.14	0.53
40G	7	417	158	44			250	2	270	15	1.19	0.89
41G	8	263	172	13			82	1	90	0	1.14	0.89
42G	6	57	349	47			248	10			1.04	0.44
52G	5	2784	166	26	180	7	73	6	90	0	1.42	0.36
57G	12	450	208	13	(353)	(8)	116	9	(290)	(7)	1.22	0.62

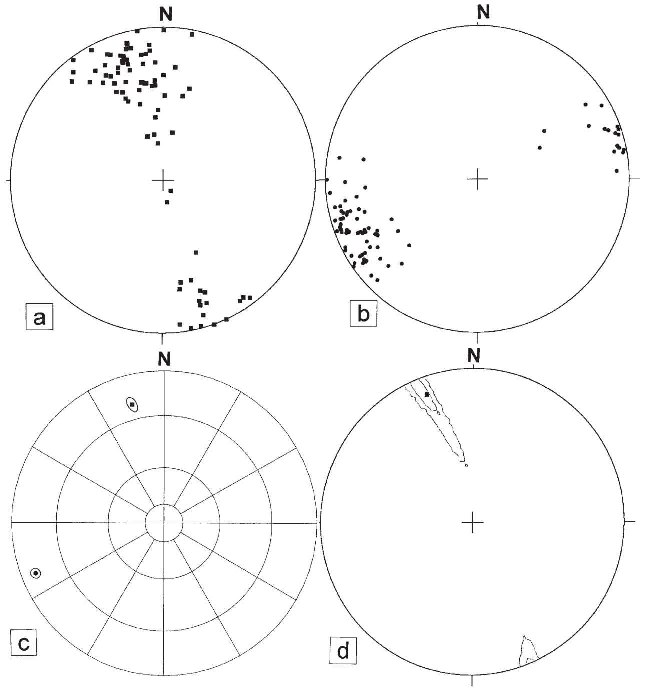

Fig. 4. All sites except 57G: (a) maximum and (b) minimum susceptibility axes. (c) Confidence zones at 95% associated with maximum and minimum susceptibility axes. (d) Magnetic zone axis (Henry, 1997), with associated confidence zones at 63 and 95%. Equal area projection in the lower hemisphere.

confidence zone remains of moderate size. The mean pole of the visible foliation (Fig. 8c) seems to be very close to this confidence zone for minimum susceptibility axis, but it is not possible, because of the deformation of the visible foliation, to determine if a significant difference exists between them. Contrary to the minimum susceptibility axes, the maximum susceptibility axes are scattered, and their associated confidence zone is very large. The mean maximum axis is close to the horizontal and thus very different from the axis of the fold affecting the visible foliation. It is therefore not really related to this local late folding.

The magnetic zone axis (Fig. 8b) has, contrary to the mean maximum axis, an associated confidence zone of moderate size. It plunges steeply and probably corresponds to the strongly plunging fold axis affecting the visible foliation in this site. The moderate scattering of the minimum axes should be therefore in relation with this folding. The magnetic zone axis is clearly different from the mean maximum axis. The maximum axes are then not really related to the variability of the magnetic foliation and are in relation to stretching of the rock. However, they do not coincide with the lineation visible in this site (Fig. 8c). The observed scattering of the maximum axes roughly around part of a vertical plane, including the magnetic zone axis, is then probably simply due to the superimposition of the effects of different events in this site, from the acquisition of the initial fabric to the local late folding during the same

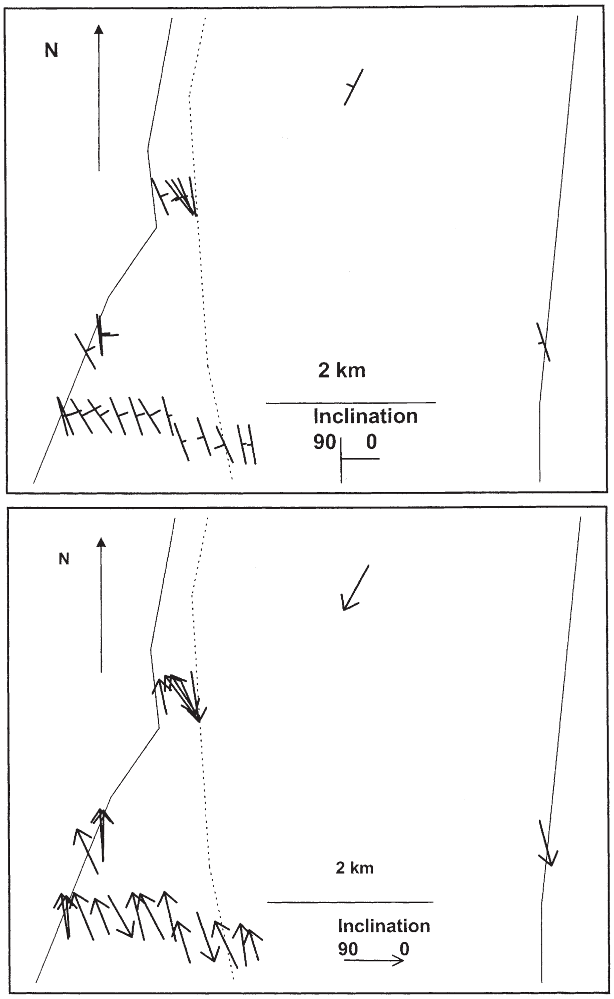

Fig. 5. Magnetic foliation and lineation.

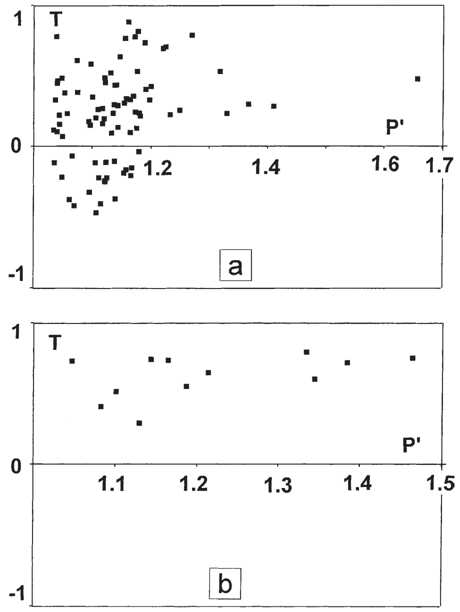

Fig. 6. P' T (Jelinek, 1981) diagram (a) for all the sites except site 57G and (b) for site 57G.

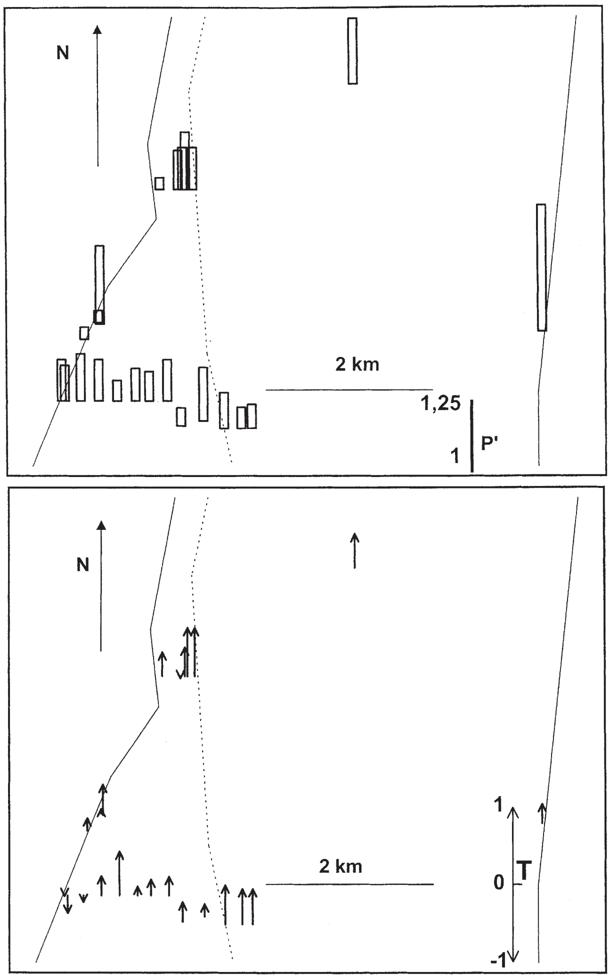

Fig. 7. P' and T values.

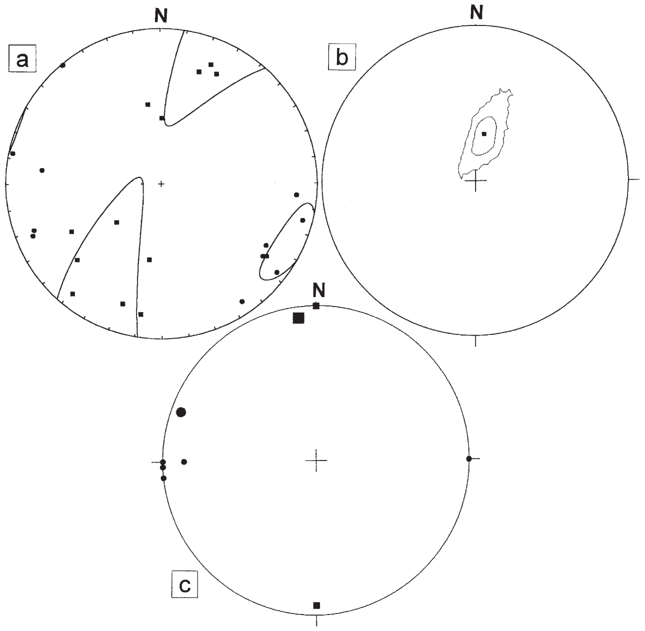

Fig. 8. Site 57G: (a) maximum (squares) and minimum (circles) susceptibility axes with associated confidence zones at 95% (Hext, 1963; Jelinek, 1978). (b) Magnetic zone axis (Henry, 1997) with associated confidence zones at 63 and 95%. (c) Mean poles of the visible foliation (circles) and visible lineation measured, because of bad outcrop conditions, in different parts of the site 57G (large symbols) and in the sites close to the faulted zone (small symbols). Equal area projection in the lower hemisphere.

tectonic phase: composite magnetic fabric, corresponding mainly to initial and stretching lineations scattered by the folding, and to fold axis lineation.

5. Discussion

5.1. Comparison with visible structures

Two different cases have been found in previous studies of sheared granites. Aranguren et al. (1996) obtained a composite fabric with a magnetic foliation in an intermediate orientation between the S and C planes. In that case, for the highest degrees of shear, the foliation is closer to the C plane. The granite has a magnetic fabric mainly related to paramagnetic minerals. Tomezzoli et al. (2003) found a magnetic foliation related to the C planes in a granite, whose magnetic fabric is mainly carried by ferromagnetic minerals. They observed a concentration of opaque minerals in these C planes.

In the Alous-En-Tides granite, the relations between magnetic and visible fabrics are different from those cited in the previous paragraph. Observations in thin sections in the deformed granite reveal weak concentrations of opaque minerals in the S planes, and to a lesser extent in the C planes. In the undeformed granite, the few opaque minerals are only visible in the S planes. In both facies, no other concentrations of opaque minerals have been observed. The magnetic fabric orientation is almost the same in the deformed and the undeformed facies, but the magnetic foliation corresponds neither to S or C planes, nor to a composite foliation between the S and C planes. The magnetic anisotropy is, however, very strong and carried by magnetite. It has a very coherent orientation in the whole study area (except within the mylonitized zone). That implies strong orientation of the magnetite crystals. The mean magnetic lineation (shallowly plunging towards NNW) is slightly different from the visible lineation (mostly horizontal N–S-trending). The magnetic fabric cannot be correlated with any preferred orientation or concentration of opaque or other minerals visible on the field and in thin sections, and is therefore carried by oriented magnetite disseminated within the rock. It seems hardly possible that such a strong magnetic fabric could be related to deformation at solid state without evidence of effects on the other minerals except cataclasis. The magnetic fabric then corresponds to structures related to deformation acquired from magmatic to sub-magmatic state.

5.2. Comparison with the magnetic fabric of 'Taourirt' granites

Djouadi and Bouchez (1992) and Djouadi et al. (1997) studied the magnetic fabric of Late Panafrican plutons in the northern part of the Hoggar. The plutons are located west of the 4°50 shear zone but not very close to it. Their fabric has many similar characteristics to that of our pluton: maximum and minimum susceptibility axes relatively well grouped around sub-horizontal directions, fabric mostly oblate. The mean orientation of the axes is different according to the plutons. On the border of the plutons, the orientation of the magnetic foliation is often relatively similar to that of the contact between plutons and host rocks. The magnetic foliation and lineation correspond to the structures locally visible in part of these plutons. The P' values are lower than in our pluton. The authors proposed that the Taourirt plutons intruded in shear zones, the conditions of emplacement of the magma, reflected by the magnetic fabric, being related to the variations of the stress field in this area.

In our pluton, the visible foliation and lineation are well defined within and on the border of the shear zone (Fig. 8c). A first major difference with the results from the Taourirt granites is that our magnetic foliation and lineation are always slightly different from their visible equivalents, except perhaps for part of the magnetic foliation in the site 57G. They are therefore mainly related to another event than that which gave rise to the visible structures. A second difference is that our magnetic fabric seems unrelated to the orientation of the contact with the Panafrican host rocks. This could indicate, for our study, fabric not really related to the actual emplacement of the magma. The main known difference in the emplacement conditions is that our pluton intruded within one of the main Late Panafrican shear zones. The stress field along this fault zone was probably much more important than in the area studied by Djouadi and Bouchez (1992) and Djouadi et al. (1997).

5.3. Emplacement conditions

Most of our sites correspond to undeformed granite. In the area with visible macrostructures, the foliation and lineation are related to a deformation at solid state with partial recrystallization and probably granite was here also massive before this deformation. Therefore the main minerals of the granite crystallized under not strongly oriented compressions. In such a shear zone, local relative distension can occur because of irregularity of the fault geometry. Displacement can then generate limited volume which is protected from regional compression, like sedimentary 'pull-apart' basins in shear zones (Djouadi et al., 1997).

5.4. Late magmatic conditions and stress-controlled crystallization

The magnetic fabric indicates strong stress in the late magmatic state. It reflects the stress field during crystallization (or recrystallization?) of magnetite (Pignotta and Benn, 1999; Benn et al., 2001; Callahan and Markley, 2003), which occurred here relatively late in the magma evolution. The pluton was at this period submitted to the regional stress field, probably after new strike-slip movements along the 7°30 shear zone. The magnetic fabric therefore reveals the ENE–WSW orientation (with gently NNW dipping stretching direction) of the regional stress field during the Late Panafrican times. A stress field with such an orientation would give dextral movements along the N–S 7°30 structure, with relative uplift of the eastern block as observed here (eastern block shows deeper metamorphic facies than the western block).

5.5. Later deformation

The visible S/C structures and stretching lineation have been clearly observed only in the sheared zone or close to this zone. Except in site 57G, the foliation is parallel to the main faults and the lineation is subhorizontal. They have been acquired during deformation related to dextral movement along the 7°30 structure. The displacement direction was subhorizontal.

The magnetic fabric is similar in this deformed area and in the other parts of the pluton without visible foliation and lineation. In particular, except for one site, P' values are almost the same. However, if P' is plotted as a function of the mean susceptibility (Henry, 1980), a clear difference appears (Fig. 9). The increase of P' as a function of the susceptibility is much stronger in the deformed area. However, no new magnetite was formed because the mean susceptibility is not higher in the deformed area. Later deformation therefore affected the magnetic fabric. These changes appear only by a slight deviation of the magnetic foliation and lineation towards their visible equivalents and by a weak increase of the oblateness and of the intensity of the fabric. This suggests that the pure shear was probably the dominant deformation during the formation of the visible structures, maybe because of the orientation of the regional compression. The weak effect of this flattening on the orientation of the magnetic foliation can be explained by the moderate difference between the magnetic fabric before deformation and the visible fabric, and above all by the fact that the fabric of the main minerals was probably without preferred orientation before deformation. In this case, deformation by flattening does not imply large grain rotation within the rock.

In site 57G, the visible foliation and lineation were themselves deformed during another step of the transcurrent regional movement. The magnetic foliation is similar to the mean visible foliation, but precise comparison cannot be made because of local folding. The magnetic lineation is different from the axis of the folds, the visible lineation and the magnetic lineation in the other sites. The relatively high scattering of the susceptibility axes and of the P' values

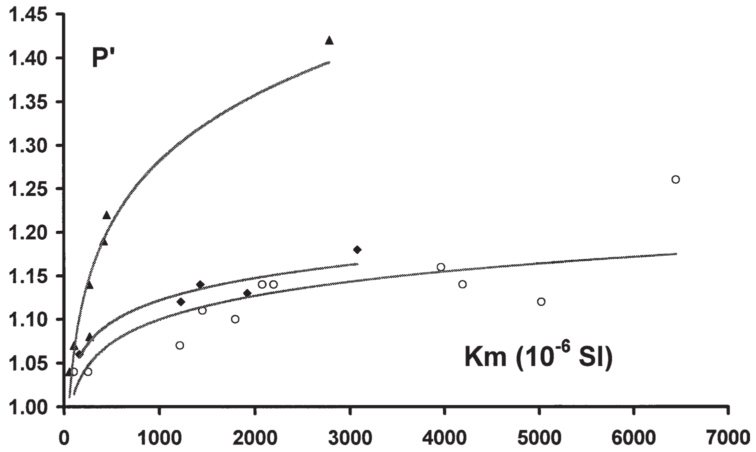

Fig. 9. Mean values by site of P' as a function of the mean susceptibility K_m in undeformed (open circles), very slightly oriented (full diamonds) and strongly deformed (full triangles) granite. The curves are only presented to underline the main trends.

could indicate in this site a more complex fabric, reflecting different events. The local folding could correspond to the last visible effect of Late Panafrican transcurrent kinematics characterized here by dextral movements along the 7°30 shear zone. Previous visible effects of this phase should have allowed pluton emplacement and should be deformation at solid state during its culmination.

6. Conclusion

Magnetic fabric cannot be related here to any visible macrostructure, but indicates a very coherent and well-defined preferred shape orientation of the magnetite. In exceptional conditions, such as a change of stress field during the end of the magmatic state of granite, the magnetic fabric can thus point out fabrics totally missed by the classical structural analyses. In the Alous-En-Tides granite, the magnetic fabric reveals in this way the late Panafrican regional stress field at the origin of the dextral movements along the 7°30 structure. The movements favored first the emplacement by intrusion of the pluton in a pull-apart zone, but put the granite under this compression field during late magmatic stages, causing the orientation of the magnetite. They later yielded strong deformation at solid state during the culmination of this Late Panafrican phase.

Acknowledgements

This project is supported by the CMEP program 01MDU521. K. Benn and G. Gleizes provided detailed and insightful comments that greatly improved the paper. We are very grateful to French Ministère des Affaires Etrangères for travel support to Algeria for one of us and to the civil and military authorities at Tamanrasset and In Azzaoua for their constant and important help in the field.

References

Aranguren, A., Cuevas, J., Tubia, J.M., 1996. Composite fabrics from S–C mylonites. Journal of Structural Geology 18, 863–869.

Benn, K., Paterson, S.R., Lund, S.P., Pignotta, G.S., Kruse, S., 2001. Magmatic fabrics in batholiths as markers of regional strain and plate kinematics: example of the Cretaceous Mt. Stuart Batholith. Physics and Chemistry of the Earth (A) 26, 343–354.

Bertrand, J.M., Caby, R., Ducrot, J., Lancelot, J.R., Moussine-Pouchkine, A., Saadallah, A., 1978. The late Pan-African intracontinental linear fold belt of the eastern Hoggar (Central Sahara, Algeria): geology, structural development, U/Pb geochronology, tectonic implications for the Hoggar shield. Precambrian Research 7, 349–376.

Black, R., Latouche, L., Liégeois, J.P., Bertrand, J.M., 1994. Pan African displaced terranes in the Tuareg shield (central Sahara). Geology 22, 641–644.

Boissonnas, J., 1973. Les granites à structures concentriques et quelques autres granites tardifs de la chaîne pharusienne en Ahaggar (Sahara central, Algérie). Thesis, University of Paris. Mémoire du Centre de Recherche sur les Zones Arides, sér. Géologie 16, 662pp.

Boissonnas, J., Duplan, L., Maisonneuve, J., Vachette, M., 1964. Etude géochronologique de roches du compartiment suggarien du Hoggar central, Algérie. Annales de la Faculté des Sciences de Clermont, 25. Géol. Min. 8, 73–90.

Caby, R., 1967. Existence du Cambrien à faciès continental («série pourprée» «Nigritien») et importance du volcanisme et du magmatisme de cet âge au Sahara central. Comptes Rendus de l'Académie des Sciences, Paris, D 264, 1386–1389.

Caby, R., 1987. The Pan-African belt of west Africa from the Sahara Desert to the Gulf of Benin. In: Schaer, J.P., Rodgers, J. (Eds.), Anatomy of Mountain Ranges, Princeton University Press, Princeton, New Jersey, pp. 129–170.

Caby, R., Moussu, H., 1967. Une grande série détritique du Sahara: stratigraphie, paléogéographie et évolution structurale de la série "pourprée" dans l'Aseg'rad et le Tanezrouft orientale (Sahara algérien). Bulletin de la Société Géologique de France IX, 876–882.

Caby, R., Bertrand, J.M., Black, R., 1981. Pan-African closure and continental collision in the Hoggar-Iforas segment, central Sahara. In: Kröner, A., (Ed.), Precambrian Plate Tectonics, Elsevier, pp. 407–434.

Cahen, L., Snelling, N.J., Delhal, J., Vail, J.R., 1984. The Geochronology and Evolution of Africa, Clarendon Press, Oxford, 512pp.

Callahan, C.N., Markley, M.J., 2003. A record of crustal-scale stress; igneous foliation and lineation in the Mount Waldo Pluton, Waldo County, Maine. Journal of Structural Geology 25, 541–555.

Cheilletz, A., Bertrand, J.M., Charoy, B., Moulahoum, O., Bouabsa, L., Farrar, E., Zimmermann, J.L., Dautel, D., Archibald, D.A., Boullier, A.M., 1992. Géochimie et géochronologie Rb/Sr, K/Ar et ^{39}Ar ^{40}Ar des complexes granitiques panafricains de la région de Tamanrasset (Algérie): relation avec les minéralisations Sn-W associées et l'évolution tectonique du Hoggar Central. Bulletin de la Société Géologique de France 163, 733–750.

Day, R., Fuller, M., Schmidt, V.A., 1977. Hysteresis properties of titanomagnetites: grain size and compositional dependence. Physics of Earth and Planetary Interiors 13, 260–267.

Djellit, H., Henry, B., Derder, M.E.M., 2002. Sur la présence d'une série molassique (de type série pourprée) au Sud-Est de l'Ahaggar (In Guezzam, Ahaggar, Algérie). Comptes Rendus Geosciences 334, 789–794.

Djouadi, M.T., Bouchez, J.L., 1992. Structure étrange du granite du Tesnou (Hoggar, Algérie). Comptes Rendus de l'Académie des Sciences, Paris 315(II), 1231–1238.

Djouadi, M.T., Gleizes, G., Ferré, E., Bouchez, J.L., Caby, R., Lesquer, A., 1997. Oblique magmatic structures of two epizonal granite plutons, Hoggar, Algeria: late orogenic emplacement in a transcurrent orogen. Tectonophysics 279, 351–374.

Henry, B., 1980. Contribution à l'étude des propriétés magnétiques de roches magmatiques des Alpes: conséquences structurales, régionales et générales. Thesis, University of Paris, 528pp.

Henry, B., 1997. The magnetic zone axis: a new element of magnetic fabric for the interpretation of the magnetic lineation. Tectonophysics 271, 325–329.

Hext, G., 1963. The estimation of second-order tensors, with related tests and designs. Biometrika 50, 353.

Jelinek, V., 1978. Statistical processing of magnetic susceptibility measured in groups of specimens. Studia Geophysica Geodetica 22, 50–62.

Jelinek, V., 1981. Characterization of the magnetic fabric of rocks. Tectonophysics 79, 63–67.

Joulia, F., 1959. Précision sur la discordance cambro-ordovicienne d'In Azzaoua (Niger). Comptes Rendus sommaire de la Société Géologique de France, 177–178.

Lelubre, M., 1952. Recherches sur la géologie de l'Ahaggar central et occidental. Thesis, University of Paris. Bulletin de Service de la Carte Géologique d'Algérie 2, 22, 739pp.

Liégeois, J.P., Black, R., Navez, J., Latouche, L., 1994. Early and late Pan-African orogenies in the Aïr assembly of terranes (Tuareg shield, Niger). Precambrian Research 67, 59–66.

Paquette, J.L., Caby, R., Djouadi, M.T., Bouchez, J.L., 1998. U–Pb dating of the end of the Pan-African orogeny in the Tuareg shield: the post-collisional syn-shear Tioueine pluton (Western Hoggar, Algeria). Lithos 45, 245–253.

Pignotta, G.S., Benn, K., 1999. Magnetic fabric of the Barrington Passage pluton, Meguma Terrane, Nova Scotia: a two-stage fabric history of syntectonic emplacement. Tectonophysics 307, 75–92.

Tomezzoli, R.N., McDonald, W.D., Tickyj, H., 2003. Composite magnetic fabrics and S–C structure in granitic gneiss of Cerro de los Viejos, La Pampa province, Argentina. Journal of Structural Geology 25, 159–169.